



ALMA MATER STUDIORUM  
UNIVERSITÀ DI BOLOGNA

ARCHIVIO ISTITUZIONALE  
DELLA RICERCA

## Alma Mater Studiorum Università di Bologna Archivio istituzionale della ricerca

Effect of pulsed electric field treatment on water distribution of freeze-dried apple tissue evaluated with DSC and TD-NMR techniques

This is the final peer-reviewed author's accepted manuscript (postprint) of the following publication:

*Published Version:*

Tylewicz, U., Aganovic, K., Vannini, M., Toepfl, S., Bortolotti, V., DALLA ROSA, M., et al. (2016). Effect of pulsed electric field treatment on water distribution of freeze-dried apple tissue evaluated with DSC and TD-NMR techniques. *INNOVATIVE FOOD SCIENCE & EMERGING TECHNOLOGIES*, 37(C), 352-358 [10.1016/j.ifset.2016.06.012].

*Availability:*

This version is available at: <https://hdl.handle.net/11585/568408> since: 2016-11-18

*Published:*

DOI: <http://doi.org/10.1016/j.ifset.2016.06.012>

*Terms of use:*

Some rights reserved. The terms and conditions for the reuse of this version of the manuscript are specified in the publishing policy. For all terms of use and more information see the publisher's website.

This item was downloaded from IRIS Università di Bologna (<https://cris.unibo.it/>).  
When citing, please refer to the published version.

(Article begins on next page)

This is the final peer-reviewed accepted manuscript of:

*Urszula Tylewicz, Kemal Aganovic, Marianna Vannini, Stefan Toepfl, Villiam Bortolotti, Marco Dalla Rosa, Indrawati Oey, Volker Heinz, **Effect of pulsed electric field treatment on water distribution of freeze-dried apple tissue evaluated with DSC and TD-NMR techniques**, Innovative Food Science & Emerging Technologies, Volume 37, Part C, 2016, Pages 352-358, ISSN 1466-8564*

The final published version is available online at:

<https://doi.org/10.1016/j.ifset.2016.06.012>

Rights / License:

The terms and conditions for the reuse of this version of the manuscript are specified in the publishing policy. For all terms of use and more information see the publisher's website.

*This item was downloaded from IRIS Università di Bologna (<https://cris.unibo.it/>)*

***When citing, please refer to the published version.***

## Accepted Manuscript

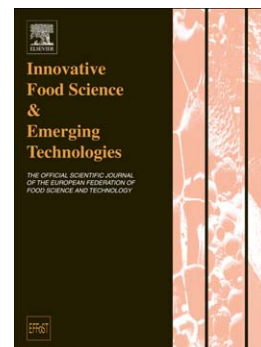
Effect of pulsed electric field treatment on water distribution of freeze-dried apple tissue evaluated with DSC and TD-NMR techniques

Urszula Tylewicz, Kemal Aganovic, Marianna Vannini, Stefan Toepfl, Villiam Bortolotti, Marco Dalla Rosa, Indrawati Oey, Volker Heinz

PII: S1466-8564(16)30117-5  
DOI: doi: [10.1016/j.ifset.2016.06.012](https://doi.org/10.1016/j.ifset.2016.06.012)  
Reference: INNFOO 1551

To appear in: *Innovative Food Science and Emerging Technologies*

Received date: 17 October 2015  
Revised date: 2 June 2016  
Accepted date: 14 June 2016



Please cite this article as: Tylewicz, U., Aganovic, K., Vannini, M., Toepfl, S., Bortolotti, V., Rosa, M.D., Oey, I. & Heinz, V., Effect of pulsed electric field treatment on water distribution of freeze-dried apple tissue evaluated with DSC and TD-NMR techniques, *Innovative Food Science and Emerging Technologies* (2016), doi: [10.1016/j.ifset.2016.06.012](https://doi.org/10.1016/j.ifset.2016.06.012)

This is a PDF file of an unedited manuscript that has been accepted for publication. As a service to our customers we are providing this early version of the manuscript. The manuscript will undergo copyediting, typesetting, and review of the resulting proof before it is published in its final form. Please note that during the production process errors may be discovered which could affect the content, and all legal disclaimers that apply to the journal pertain.

**Effect of pulsed electric field treatment on water distribution of freeze-dried apple tissue  
evaluated with DSC and TD-NMR techniques**

**Urszula Tylewicz<sup>a,b\*</sup>, Kemal Aganovic<sup>c</sup>, Marianna Vannini<sup>d,e</sup>, Stefan Toepfl<sup>c</sup>, Villiam  
Bortolotti<sup>d,e</sup>, Marco Dalla Rosa<sup>a,b</sup>, Indrawati Oey<sup>f,g</sup>, Volker Heinz<sup>b</sup>**

<sup>a</sup> *Department of Agricultural and Food Sciences, University of Bologna, Campus of Food Science,  
Cesena, Italy*

<sup>b</sup> *Interdepartmental Centre for Agri-Food Industrial Research, University of Bologna, Cesena, Italy*

<sup>c</sup> *German Institute of Food Technologies (DIL e.V.), Quakenbrueck,, Germany*

<sup>d</sup> *Interdepartmental Centre of Energy and Environment, University of Bologna, Bologna, Italy*

<sup>e</sup> *Department of Civil, Environmental, Materials and Chemical Engineering, University of Bologna,  
Bologna, Italy*

<sup>f</sup> *Department of Food Science, University of Otago, Dunedin, New Zealand*

<sup>g</sup> *Riddet Institute, Palmerston North, New Zealand*

\*Corresponding author: Tel. +39 0547338120; e-mail: urszula.tylewicz@unibo.it; postal  
address: Department of Agricultural and Food Sciences, Campus of Food Science,  
University of Bologna; Piazza Goidanich, 60; 47521 Cesena (Italy)

**Abstract**

This work aimed to study pulsed electric fields (PEF) effect on the water distribution of freeze-dried apple. Apple (*var.* Cripps Pink) was treated in 15% trehalose and 1% ascorbic acid solution (388  $\mu\text{S}/\text{cm}$ ) at 3 Hz and various electric field strengths 0.3; 0.6; 0.9 and 1.2 kV/cm for 5, 10 or 15 pulses. The samples were frozen at  $-45^{\circ}\text{C}$  and freeze-dried. The analyses were performed after rehydration. Differential Scanning Calorimetry (DSC) and Nuclear Magnetic Resonance in the domain of time (TD-NMR) were performed to assess thermal properties of freezable water and water distribution in apple tissue, respectively. PEF changed the integrity and continuity of the cell structure shown by the water redistribution between different compartments. The water in vacuoles and extracellular spaces had higher TD-NMR relaxation times as water molecules can diffuse in larger volumes before relaxing, even if the overall solutes concentration in the tissue increases.

**Key words:** Pulsed electric fields; freeze-drying; apple; water distribution; DSC; TD-NMR.

## 1. Introduction

Freeze-drying is widely used to dry fruit and vegetables. This technique is based on dehydration by sublimation of previously frozen tissues. It offers advantages such as increasing rehydration rate, maintaining the shape and the volume of plant tissues and increasing microbial stability (Ratti, 2001). Due to the formation of ice during the freezing process, the tissue collapse after the rehydration process was reported (Lewicki & Wiczowska, 2007). Since the freeze-dried products are usually consumed after rehydration, understanding the mechanisms of mass transfer (water and soluble solids) occurring during rehydration is of the key importance (Mastrocola, Dalla Rosa, & Massini, 1997). In order to improve qualitative and nutritional characteristics and to reduce the time of freeze-drying process, the application of several pre-treatments before freeze-drying has been studied as for example blanching (Doymaz, 2010), osmotic dehydration (Cieurzyńska & Lenart, 2010) and infrared heating (Pam, Shih, McHugh, & Hirschberg, 2008).

In the last years the use of pulsed electric fields (PEF) technology for food processing has been studied. PEF treatment leads to electroporation of the cell membrane by applying an external electric field to the cellular tissue (Zimmerman, Pilwat, & Riemann, 1974; Zimmerman, 1996). Electroporation of the cell membranes could promote reversible or irreversible pore formation and cell disintegration, depending on both the intensity of the electric field strength applied and the characteristics of the raw materials (Angersbach, Heinz, & Knorr, 2000; Puc, Corovic, Flisar, Petkovsek, Nastran, & Miklavcic, 2004; Dymek, Dejmek, & Gómez Galindo, 2014; Toepfl, Siemer, & Heinz, 2014). Cell disintegration can be measured based on changes in the conductivity (De Vito, Ferrari, Lebovka, Shynkaryk, & Vorobiev, 2008; Ben Ammar, Lanoisellé, Lebovka, Van Hecke, & Vorobiev, 2011). PEF processing offers several advantages i.e. to improve extraction process (Luengo, Álvarez, & Raso, 2013; Barba, Galanakis, Esteve, Frigola, & Vorobiev, 2015), to enhance mass transport phenomena (Vorobiev & Lebovka, 2010; Donsi, Ferrari, & Pataro, 2010; Wiktor, Iwaniuk, Śledź, Nowacka, & Chudoba, & Witrowa-Rajchert, 2013), and to inactivate enzymes (Elez-Martínez, Suárez-Recio & Martín-Belloso, 2007) and microorganisms (Saldaña, Puértolas, López, García, Álvarez, & Raso, 2009; Timmermans, Nierop Groot, Nederhoff, van Boekel, Matser & Mastwijk, 2014).

PEF treatment prior to drying process seems to have an effect on rehydration capacity of the resulting dried samples. Some authors reported an increase in rehydration rate (Esthiaghi, Stute, & Knorr, 1994), but some authors reported an inverse phenomenon, i.e. a decrease in rehydration rate (Taiwo, Angersbach, & Knorr, 2002; Ade-Omowaye, Angersbach, Taiwo, & Knorr, 2001) or no change in the constant rate of rehydration in both control and PEF treated samples (Gachovska, Simpson, Ngadi, & Raghavan, 2008). So far, the aforementioned conflicting phenomena are not

well understood and they require further investigation using advanced methodology to investigate the water distribution and movement in heterogeneous matrix such as plant materials after PEF pretreatment.

Foods are proton-rich due to the presence of water, fat, carbohydrates or proteins.  $^1\text{H}$  Nuclear Magnetic Resonance ( $^1\text{H}$  NMR) in the time domain (TD-NMR) is a powerful non-invasive and non-destructive technique already commonly used to investigate the composition and internal structure of foods. TD-NMR can also monitor the compositional and structural modifications when foods undergo natural or artificial processes. Hence this technique can be used to investigate internal variations in the water content, as well as changes in the water interaction with cellular tissues (Butz, Hofmann, & Tauscher, 2005). During TD-NMR measurement, these variations are examined by studying the relaxation times parameters, i.e.  $T_1$  (spin-lattice or longitudinal relaxation) and  $T_2$  (spin-spin or transverse relaxation). In general,  $T_1$  and  $T_2$  are complex distributions of relaxation times and are commonly used to monitor the structural changes in foods during processing and storage (Marcone, Wang, Alabish, Nie, Somnarain, & Hill, 2013).

Recently TD-NMR has been employed to investigate the cell walls and membrane disruption and water mobility in the plant tissue subjected to PEF treatment (Ersus, Oztop, McCarthy, & Barrett, 2010; Aguiló-Aguayo, Downey, Keenana, Lyng, Brunton, & Rai, 2014). Ersus et al. (2010) were able to follow the changes of  $T_2$  relaxation times from two different cell compartments namely cytoplasm and vacuoles. They showed that the  $T_2$  values were strongly correlated with ion leakage from the onion tissue. Aguiló-Aguayo et al. (2014) investigated the water distribution in carrot slices after PEF treatment, showing the alteration of cell membrane and vacuoles which caused changes in  $T_2$  as a consequence of water redistribution between cellular structures. TD-NMR technique has been successfully used to explore the effect of osmotic dehydration on water mobility in terms of signal intensity and the  $T_2$  relaxation of protons separately for vacuoles, cytoplasm/extracellular spaces and cell wall of different fruits (Cheng, Zhang, Adhikari, & Islam, 2014; Marigheto, Venturi & Hills, 2008; Tylewicz et al., 2011; Dalla Rosa et al., 2011; Panarese; Laghi, Pisi, Tylewicz, Dalla Rosa, & Rocculi, 2012; Santagapita, Laghi, Panarese, Tylewicz, Rocculi, & Dalla Rosa, 2013). In addition, Magnetic Resonance Imaging can be used for non-destructive evaluation of the internal structure of different food systems (Bortolotti, Fantazzini, Gombia, Greco, Rinaldin, & Sykora, 2010; Defreye et al., 2013) on the basis of gas, water and solutes exchange. In general, most studies use  $T_2$  as a parameter because it is easily measured however  $T_1$  is a robust parameter that can well describe foods properties and structural modifications.

The aim of this work was to investigate the effects induced by PEF pre-treatment at different electric field strengths on the water distribution in freeze-dried apple tissue using both DSC and TD-NMR. In this work, TD-NMR  $T_1$  analysis was applied on rehydrated apple tissue to detect variations in the water state of the cellular tissue treated with PEF processing.  $T_2$  analysis was additionally performed to evaluate potential water diffusion effects. To investigate the water-solid exchange followed by different food processing, Differential Scanning Calorimetry (DSC) was used. Different authors investigated the changes in freezable water content by DSC technique during fruit ripening (Goñi, Muñoz, Ruiz-Cabello, Escribano, & Merodio, 2007), osmotic dehydration (Tylewicz et al, 2011; Cheng et al., 2014) and freeze-drying (Zhao, Liu, Wen, Xiao, & Ni, 2015). During rehydration of freeze-dried products several changes take place i.e. water transfer from the liquid phase, where the sample is soaked, into the food and transfer of soluble solids from the food into the liquid phase. To the best of our knowledge so far there is no information about the consequences of the PEF application prior to freeze-drying on the water state of the cellular plant tissue.

## 2. Material and Methods

### 2.1. Raw Material, Handling, and Storage

Medium-size apples var. Cripps Pink ( $15 \pm 1$  °Brix) were purchased from the local market in Quakenbrueck (Germany). The apples were stored at  $2 \pm 1$  °C at high relative humidity protected from light until use.

### 2.2. Sample Preparation

The apples were manually washed, peeled and cut into half with a sharp scalpel. Two cylindrical samples with a diameter of  $d=20$  mm, height of  $h=20$  mm and weight of about  $m=2.6$  g were cut from the inner part of the parenchyma tissue of each apple half. Immediately after cutting, the samples were weighted and placed in the PEF chamber. The treatment was performed in a solution mixture of 15% trehalose and 1% ascorbic acid having the conductivity of 388  $\mu\text{S}/\text{cm}$ .

### 2.3. Pulsed electric field (PEF) treatment

The PEF treatment was conducted using batch 5 kW generator constructed by DIL (Germany), with a voltage output range of 8-19 kV. The treatment chamber was composed of 2 stainless steel parallel electrodes. The distance between the electrodes was 8 cm with the total area of 170

cm<sup>2</sup>. The form of the chamber was rectangular prism (length: 17 cm, height: 10 cm; width: 8 cm), where the bottom of the chamber and the side holding the two electrodes were made of Polyether ether ketone (PEEK) materials as insulator.

One of the electrode was connected with high voltage current and the other was grounded.

To reach desired electric field strength, output voltage was adjusted according to the size of treatment chamber used (distance between the electrodes) and calculated using equation 1:

$$E = \frac{U}{d} \quad (1)$$

where  $E$  is electric field strength (V/cm),  $U$  is voltage (V) and  $d$  is electrode distance (cm)

Twelve cylindrical samples (total weight of 70 g) were used for each treatment. The treatment chamber was filled with trehalose/ascorbic acid solution (total weight of 650 g). The voltage output was set to achieve 0.3; 0.6; 0.9 and 1.2 kV/cm in a treatment chamber and the number of pulses (with a monopolar exponential decaying pulse shape) used for the treatments was 5, 10 and 15. The pulse width was set to 60  $\mu$ s and the frequency was fixed to 3 Hz. The parameters used in this study were selected based on the previous study of Ersus et al. (2010), as summarised in Table 1. Total energy input ( $W_{\text{whole}}$ , kJ/kg) was calculated according to equation 2.

$$W_{\text{whole}} = \frac{0.5 \cdot U^2 \cdot c}{V \cdot \rho} \cdot \eta \quad (2)$$

where  $U$  is voltage applied (V);  $c$  – capacity of the construction (F);  $V$  – volume of treatment chamber (m<sup>3</sup>);  $\rho$  – product density (kg·m<sup>-3</sup>) and  $\eta$  – number of pulses used for treating the product. All the treatments were performed at room temperature.

After PEF treatment, the samples were removed from the solution, placed on blotting paper (to remove the surface water) and weighted. Afterwards the untreated and PEF-treated samples were cut lengthways into half, frozen at -45°C and freeze-dried.

#### 2.4. Cell disintegration index ( $Z_p$ )

The electrical conductivity was measured before and immediately after the PEF treatment. The cylindrical apple samples ( $d=20$  mm,  $h=20$  mm) were placed between two stainless steel electrodes of the conductivity meter (DIL, Germany). The cell disintegration index was calculated according to equation 3.

$$Z_p = 1 - \frac{K_h}{K'_h} \cdot \frac{(K'_h - K'_l)}{(K_h - K_l)} \quad (3)$$

where  $K_l$ ,  $K'_l$  are the electrical conductivity of fresh and treated samples, respectively, in a low-frequency (1-5 kHz);  $K_h, K'_h$  are the electrical conductivity of fresh and treated samples, respectively, in a high-frequency (3-50 MHz) (Knorr & Angersbach, 1998). The values of this index ranged from 0 to 1, where  $Z_p=0$  stands for an intact tissue and  $Z_p=1$  is for maximally disintegrated one. The measurement of electrical conductivity was performed in four replications and the results are expressed as a mean value of cell disintegration index.

### 2.5. Rehydration

The freeze-dried samples were placed inside a beaker filled with distilled water. The liquid: solid ratio was fixed to a 100:1 ratio. The rehydration process was performed at  $20 \pm 2$  °C for 15 min.

### 2.6. DSC measurements

DSC analysis was carried out using Pyris 6 DSC (Perkin-Elmer Corporation, Wellesley, USA) equipped with a low-temperature cooling unit (Intacooler II Perkin-Elmer Corporation, Wellesley, USA). Temperature and melting enthalpy calibrations were performed with ion exchanged distilled water (melting point - mp 0.0 °C), indium (mp 156.60 °C), and zinc (mp 419.47 °C); heat flow was calibrated using the heat of fusion of indium ( $\Delta H = 28.71 \text{ J} \cdot \text{g}^{-1}$ ). For the calibration, the same heating rate, as used for sample measurements, was applied under a dry nitrogen gas flux of  $20 \text{ mL} \cdot \text{min}^{-1}$ . Rehydrated samples of about 20-30 mg were encapsulated in 50  $\mu\text{l}$  hermetic aluminium pans prior to measurements. An empty pan was used as a reference. DSC curves were obtained by cooling samples to -70 °C and then heating at the rate of  $5 \text{ }^\circ\text{C} \cdot \text{min}^{-1}$  up to 100 °C after an isothermal hold for 2 min at -70 °C. According to Quinn, Kampff, Smyth, & McBrierty (1988) the amount of freezable water ( $\text{g} \cdot \text{g}_{\text{fw}}^{-1}$ ) was determined using equation 4.

$$x_w^F = \frac{\Delta H}{\Delta H_{\text{ice}}} \quad (4)$$

where  $\Delta H$  ( $\text{J} \cdot \text{g}^{-1}$ ) is the measured latent heat of melting of water for gram of sample obtained by the integration of the melting endothermic peak;  $\Delta H_{\text{ice}}$  ( $334 \text{ J} \cdot \text{g}^{-1}$ ) is the latent heat of melting of pure water at 0 °C.

## 2.7. NMR Measurements

Rehydrated half-cylinders were used for the NMR measurements. TD-NMR relaxation signal curves were acquired with a console and a 25 mm in diameter coil both manufactured by Stelar (Mede, PV, Italy) and using a permanent 0.2 T magnet (ESAOTE SpA, Genova, Italy). A standard Inversion-Recovery (IR) sequence was used to sample the  $T_1$  relaxation curves. Typical IR acquisition parameters were: free induction decay (FID) curves acquired for 128 values at different inversion time increasing in geometrical progression (in order to cover uniformly the multi-exponential relaxation curve); each FID was sampled with 512 points at steps of 4  $\mu$ s, with 16 scans for each measurement. The  $T_2$  relaxation signal curves were acquired by a standard CPMG (Carl-Purcell-Meiboom-Gill) pulse sequence with 2048 echoes, spaced with echo times of 200  $\mu$ s, 500 $\mu$ s and 1000 $\mu$ s, acquiring totally three different measurements to detect diffusion effects. The number of scans was equal to 32. For all experiments, the relaxation delay was set to a value greater than 4 times the maximum  $T_1$  of the sample, corresponding to a recycle delay of 7200 ms. All curves were acquired using phase-cycling procedures.

$T_1$  and  $T_2$  relaxation data were processed to produce quasi-continuous relaxation times distributions using the UpenWin software (Bortolotti, Brown, & Fantazzini, 2009). UpenWin is a Windows program specifically designed not to provide distribution details that are not supported by data, which might be misinterpreted, for example, as physically meaningful resolved pore compartments. Therefore, by default UpenWin basically produces smoothed distributions. In order to synthesize a complex distribution with a single more manageable value, various single parameters (or kinds of averages) can be computed from the relaxation time distribution itself. Distribution peaks position ( $T_{(1,2)p}$ ) and geometric weighted average ( $T_{(1,2)g}$ ) are among these parameters and they were used in this work for data analyses.

## 3. Result and discussion

### 3.1. Cell disintegration

In this study the  $Z_p$  index increased when increasing the applied pulse numbers and elevating the level of electric field strength at above 0.3 kV/cm. At 0.3 kV/cm, the index remained unchanged when increasing the number of pulses (Table 1). However, in most of the cases the values did not exceed 10 % indicating that electric field strength applied possibly led to low level of damage. The increase of  $Z_p$  index is strictly related to the tissue softening as discussed by De Vito et al. (2008).

The authors observed that at the  $Z_p$  index up to 0.2 the apple tissue firmness was similar to these of non-treated apples. The increase of disintegration index to 0.5 or higher promoted a high tissue softening almost compared to the freeze-thawed apple samples. The increase of this index with increasing electric field strength and pulse numbers has been also observed in carrots (Rastogi, Eshtiagi, & Knorr, 1999), potatoes (Jalté, Lanoisellé, Lebovka, & Vorobiev, 2009) and apples (Wiktor et al., 2013; Wiktor, Schulz, Voigt, Witrowa-Rajchert, Knorr, 2015). On the other hand, Ersus et al. (2010) observed that ion leakage was dependent on electric field strength applied but only at the very low voltage values. Those authors applied electric field strength of 125, 250, 500, 750, 1000, 1250, and 1500  $V\ cm^{-1}$  at 1 Hz for 10 pulses with pulse width of 100  $\mu s$  to the onion tissue and they observed that starting from 0.5 kV/cm no significant differences were observed in ion leakage in onion tissue, which means that 0.5 kV/cm was the optimal/critical values to ensure the total rupture of onion tissue cells. Moreover, the degree of tissue damage has also been found to depend on the structure of plant tissue, shape and dimension of the cells. In particular, Ben Ammar et al. (2011), applying the PEF treatment ( $E=400$  or  $1000\ V\ cm^{-1}$ , pulse width=1ms, pulse repetition=10 ms) to the different plant tissues having different size of cells, predicted higher damage for tissue with larger cells. However, they didn't find direct correlations between damage efficiency and cell size in the experimental data of the selected fruit and vegetables tissues (apple, potato, carrot, zucchini, orange and banana).

Figure 1 depicts the correlation between the cell disintegration index and total energy delivered to the apple samples. In general, the more energy delivered to the samples, the higher damage of the tissue ( $r = 0.9459$ ,  $p < 0.05$ ). Similar trend of these parameters has been observed by Wiktor et al. (2013), however in their case, the highest  $Z_p$  did not correspond to the highest energy input, suggesting that the  $Z_p$  depend not only on electric field strength and energy input but also on the pulses number.

### 3.2. DSC measurements

Differential scanning calorimetry was able to measure the initial temperature of freezing ( $T_{f_{onset}}$ ) and freezable water content. The latter comprises both free and bound water which are able to crystallize into ice, whilst unfreezable water cannot undergo any change (Cheng et al., 2014). Table 2 shows the changes of the initial freezing temperature and freezable water content of rehydrated apple samples. The application of PEF pre-treatment led to a decrease in both the initial freezing temperature and the freezable water content. The depletion of  $T_{f_{onset}}$  progressively increased along with the increasing of electric field strength applied. However, significant differences were observed only when 15 pulses were applied. Similar results were observed for freezable water

content. With increasing electric field strength, generally, the samples showed a significant decrease of freezable water content. In fact, there is a good linear correlation between freezable water contents and increasing field strengths ( $0.8013 < r < 0.9591$ ,  $p < 0.05$ ), as it can be seen in Figure 2. No significant differences ( $p < 0.05$ ) were observed in samples treated with the same electric field strength but with different pulse number. Therefore it seems that neither the initial point of freezing nor freezable water content were influenced by the number of pulses applied. The reduction of these two parameters is generally related to an increase of solute concentration and decrease of water activity within the plant tissue, which can slow down degradative reactions and guarantee a higher microbiological stability of the food products (Gianotti, Sacchetti, Guerzoni, & Dalla Rosa, 2001). According to Huang et al. (2012), freeze-drying process of apple slices did not cause any significant changes in shrinkage or cell collapse compared to the fresh samples. Even the application of PEF pre-treatment prior freeze-drying process did not promote any changes in comparison to the untreated freeze-dried potato samples (Jalté et al., 2009). The structure of polyhedral shaped cells, observed in SEM micrographs by Jalté et al. (2009), was perceptibly distorted for both untreated and PEF pre-treated samples, however no large intercellular voids were observed that is probably related to the enhanced fraction of small ice crystals inside the frozen potato tissue. In the present work a trend between damage of apple tissue, measured in terms of cell disintegration index, and freezable water content has been observed ( $r = 0.6921$ ,  $p < 0.05$ ). As it can be observed from Figure 3, an increase of cell disintegration index reflects the decrease in freezable water content. This could be because the water present in the vacuoles gets into contact with water in cytoplasm and extracellular spaces, thus an overall increase of the solute concentration can occur, which lowers the free and bound water content. In fact, the application of PEF compromises the integrity of cell membrane, tonoplast and plasma membrane which are responsible for regulation of water and solutes movement in plant cell (Vorobiev & Lebovka, 2006). Thus, there is an enhancement of fluid diffusion between extracellular and intracellular spaces, in particular the water moves from vacuoles to cytoplasm and extracellular spaces in order to equilibrate the concentrations on both sides (Zhang & McCarthy, 2012).

### 3.3. NMR measurements

As the highest modifications on cell disintegration index were observed after applying 15 pulses, NMR measurements were done only on the rehydrated samples treated with 15 pulses and different electric field strength, and on a fresh sample. In general, the  $T_1$  relaxation time distributions were bimodal, showing two well distinguished peaks. The area under the relaxation distribution curve represents the NMR proton signal. As a way of example, figure 4 shows the  $T_1$  distribution for fresh

and PEF pre-treated samples with the lowest and the highest electric field strength applied. Based on the literature (Marigheto, Vial, Wright, & Hills, 2004; Tylewicz et al., 2011; Panarese et al., 2012), the first peak in figure 4 (around 300-400 ms and occupying about 4% of the total area) could be attributed to the proton pools located in cytoplasm and extracellular spaces and the second one (around 1400 ms and occupying about 96% of the total area) to the protons located in vacuoles. Mauro et al. (2015) found three different protons populations in fresh Cripps Pink apple samples at approximately  $T_2$  values of 10, 200 and 1200 ms and were ascribed to cell wall, cytoplasm-free space and vacuole respectively. Considering the physical reasons that  $T_2$  is always less than  $T_1$ , the two higher values are in discrete agreement with our results. Instead, the proton populations corresponding to a  $T_2$  of 10 ms, the cell wall, was not observed at all.

Figure 5 shows the  $T_{1g}$  and the freezable water content versus the electric field strength. Application of electric field strength of  $0.3 \text{ kV cm}^{-1}$  produces the increase of freezable water content and decrease of  $T_1$  relaxation time, while these parameters showed the opposite behaviour when the higher electric field strength was applied. This different behaviour of the samples when very low amount of energy was provided to the samples ( $0.01\text{-}0.03 \text{ kJ kg}^{-1}$ ) could indicate that the electroporation of the tissue in this condition was reversible. In fact, in these samples the disintegration index remained at very low level (about 0.025) and was not affected at all by the pulse number applied (Table1). Analysis of  $T_{2g}$  computed on  $T_2$  curves acquired at different eco times (data not shown) did not present significant differences ( $p < 0.05$ ), this means the diffusion effects are negligible. Repetition measurements on the same samples produces discrepancy on the NMR parameters computed generally less than 5 %.

In addition to the analysis of geometric averaged times, the  $T_1$  peak positions behavior was also analyzed. Figure 6 shows the  $T_{1p}$  versus the electric field strength. It is worthy to note that the analysis of the trend of each peak position can give important information when the relaxation time distributions shows independent spin populations (or in other words, multimodality). In fact, while the geometric weighted average times describe the behavior of the whole spin population, the relaxation time peaks are related to different populations separately. Figure 6 shows the plotting of both trends of the  $T_{1p}$  of the peaks at long relaxation times and at short relaxation times.

As illustrated in figure 6, the  $T_{1p}$  at long relaxation times is almost the same considering the error, whereas the highest changes regard the short  $T_{1p}$  that corresponds to the cytoplasm/extracellular proton pools. This could indicate that tonoplast integrity was compromised increasing the exchange of water between cell vacuole and extracellular/cytoplasm volumes; some water from extracellular/cytoplasm spaces can move in the vacuole volumes and vice versa producing an appreciable increase in the  $T_1$  of the water in extracellular/cytoplasm volumes. This is in accordance

with the difference in the amount of the NMR signal (or in other word in the amount of water) associated to the two peaks. Being the quantity of water in vacuole substantially more than extracellular/cytoplasm water, the variation of its NMR relaxation times due to the contact is less evident.

Aguiló-Aguayo et al. (2014), working with  $T_2$  relaxation times observed the overlapping of peaks corresponded to above mentioned compartments and the overall reduction of  $T_2$  relaxation times with increasing electric field strength applied. However, the intensity of PEF treatment was higher compared to the one applied in this study and the water mobility was studied immediately after PEF treatment and not after rehydration of freeze-dried samples. Furthermore, Ersus et al. (2010) observed the decrease of  $T_2$  relaxation time with increasing PEF treatment, but in freeze-thawed onion cells, which is known to be a destructive process for the cell integrity.

In summary, it is possible to observe that, especially for the  $T_1$  short peak positions,  $T_1$  shows a trend that increases with increasing the electric field strength. This trend is opposite to that shown by the amount of freezable water that decreases when electric field strength increases. The possible explanation of this behavior is an increase of some cell spaces (the reduction of integrity of plasma membrane) and, even if the concentration of the solution increases, therefore reducing the freezable water, the water has a larger space available before relaxing, therefore increasing the relaxation times.

#### 4. Conclusions

The PEF treatment under the condition used in this study affected the cell integrity. It shows the progressive increasing of cell disintegration index with an increase of electric field strength, pulse numbers and energy delivered to the samples. PEF pre-treatment prior freeze-drying process promoted the reduction of the initial freezing temperature and freezable water content in the whole rehydrated tissue, indicating an increase of overall concentration of solution.

TD-NMR analysis gave more microscopic information about changes of water mobility in the singular cell compartments. In general, a well-defined increasing trend in  $T_1$  relaxation times for the extracellular spaces compartments was observed with higher intensity of PEF pre-treatment. PEF treatment compromised the integrity and continuity of the cell structure (increase of  $Z_p$  index), thus in general the water can diffuse in larger volumes before relaxing, increasing the relaxation times. Further studies and measurements are needed to better understand the effect of PEF treatment on water mobility phenomena, and how it could be related to the product quality and stability.

**Acknowledgement**

Urszula Tylewicz would like to acknowledge the Cost Action TD 1104 for receiving the Short Term Scientific Mission (STSM) grant at the German Institute of Food Technologies. Research work was also supported by POR-FESR 2007-2013 Emilia-Romagna Region. Indrawati Oey would like to thank Royal Society funding for NZ-Germany Science and Technology Programme for Non Thermal Processing (FRG13-10).

ACCEPTED MANUSCRIPT

## References

- Ade-Omowaye, B. I. O, Angersbach, A., Taiwo, K. A. & Knorr, D. (2001). Use of pulsed electric field pretreatment to improve dehydration characteristics of plant based foods. *Trends in Food Science and Technology*, 12, 285–295.
- Aguiló-Aguayo, I., Downey, G., Keenana, D. F., Lyng, J. G., Brunton, N., Rai D. K. (2014). Observations on the water distribution and extractable sugar content in carrot slices after pulsed electric field treatment. *Food Research International*, 64, 18–24.
- Angersbach, A., Heinz, V., & Knorr, D. (2000). Effects of pulsed electric fields on cell membranes in real food systems. *Innovative Food Science and Emerging Technologies*, 1, 135-149.
- Barba, F. J., Galanakis, Ch. M., Esteve, M.J., Frigola, A., & Vorobiev E. (2015). Potential use of pulsed electric technologies and ultrasounds to improve the recovery of high-added value compounds from blackberries. *Journal of Food Engineering*, 167, 38-44.
- Ben Ammar, J., Lanoisellé, J. L., Lebovka, N.I., Van Hecke, E., & Vorobiev, E. (2011). Impact of a Pulsed Electric Field on Damage of Plant Tissues: Effects of Cell Size and Tissue Electrical Conductivity. *Journal of Food Science*, 76(1), E90-E97.
- Bortolotti, V., Brown, R. J. S. & Fantazzini, P. (2009). UpenWin: a software to invert multi-exponential relaxation decay data. Distributed by the University of Bologna, [villiam.bortolotti@unibo.it](mailto:villiam.bortolotti@unibo.it).
- Bortolotti, V., Fantazzini, P., Gombia, M., Greco D., Rinaldin G., Sykora S. (2010). PERFIDI filters to suppress and/or quantify relaxation time components in multi-component systems: An example for fat–water systems. *Journal of Magnetic Resonance*, 206, 219–226.
- Butz, P., Hofmann, C. & Tauscher B. (2005). Recent developments in noninvasive techniques for fresh fruit and vegetables internal quality. *Journal of Food Science*, 70, 131–141.
- Cheng, X.-f., Zhang, M., Adhikari, B., Islam, M.N. (2014). Effect of Power Ultrasound and Pulsed Vacuum Treatments on the Dehydration Kinetics, Distribution, and Status of Water in Osmotically Dehydrated Strawberry: a Combined NMR and DSC Study. *Food and Bioprocess Technology*, 7(10), 2782-2792.
- Ciurzyńska A., Lenart A. (2010). Rehydration and sorption properties of osmotically pretreated freeze-dried strawberries. *Journal of Food Engineering*, 97, 267–274.
- Dalla Rosa, M., Tylewicz, U., Panarese, V., Laghi, L., Pisi, A. M., Santagapita, P., Rocculi, P. (2011). Effect of osmotic dehydration on kiwifruit: results of a multianalytical approach to structural study. *Journal on Processing and Energy in Agriculture*, 15(3), 113-117

- De Vito, F., Ferrari, G., Lebovka, N. I., Shynkaryk, N. V., & Vorobiev E. (2008). Pulse Duration and Efficiency of Soft Cellular Tissue Disintegration by Pulsed Electric Fields. *Food and Bioprocess Technology*, 1, 307–313.
- Defraeye, T., Lehmann, V., Gross, D., Holat, C., Herremans, E., Verboven, P., Verlinden, B.E., Nicolai B. M. (2013). Application of MRI for tissue characterization of “Braeburn” apple. *Postharvest Biology and Technology*, 75, 96-105.
- Donsi, F., Ferrari, G., & Pataro G. (2010). Applications of pulsed electric field treatments for the enhancement of mass transfer from vegetable tissue. *Food Eng. Rev.* 2(2), 109–130.
- Doymaz I. (2010). Effect of citric acid and blanching pre-treatments on drying and rehydration of Amasya red apples. *Food and bioproducts processing*, 8, 124–132.
- Dymek, K., Dejmek, P., & Gómez Galindo F. (2014). Influence of Pulsed Electric Field Protocols on the Reversible Permeabilization of Rucola Leaves. *Food and Bioprocess Technology*, 7, 761–773.
- Elez-Martínez P., Suárez-Recio M., Martín-Belloso O. (2007). Modeling the reduction of pectin methyl esterase activity in orange juice by high intensity pulsed electric fields. *Journal of Food Engineering*, 78, 184–193.
- Ersus, S., Oztop, M. H., McCarthy, M. J., & Barrett, D. M. (2010). Disintegration Efficiency of Pulsed Electric Field Induced Effects on Onion (*Allium cepa* L.) Tissues as a Function of Pulse Protocol and Determination of Cell Integrity by <sup>1</sup>H-NMR Relaxometry. *Journal of Food Science*, 75(7), E444- E451.
- Eshtiaghi, M. N., Stute, R. & Knorr D. (1994). High pressure and freezing pretreatment effects on drying, rehydration, texture and color of green beans, carrots and potatoes. *Journal of Food Science*, 59, 1168 1170.
- Gachovska, T. K., Simpson M. V., Ngadi M. O., & Raghavan G. S. V. (2009). Pulsed electric field treatment of carrots before drying and rehydration. *Journal of the Science of Food and Agriculture*, 89, 2372-2376.
- Gianotti, A., Sacchetti, G., Guerzoni, M. E., & Dalla Rosa M. (2001). Microbial aspects on short time osmotic treatment of kiwifruit. *Journal of Food Engineering*, 49, 265-270.
- Goñi, O., Muñoz, M., Ruiz-Cabello J., Escribano, M. I., Merodio C. (2007). Changes in water status of cherimoya fruit during ripening. *Postharvest Biology and Technology*, 45, 147–150.
- Jalté, M., Lanoisellé, J.-L., Lebovka, N. I., & Vorobiev E. (2009). Freezing of potato tissue pre-treated by pulsed electric fields. *LWT - Food Science and Technology*, 42, 576–580.
- Knorr, D. & Angersbach A. (1998). Impact of high-intensity electric field pulses on plant membrane permeabilization. *Trends in Food Science and Technology*, 9(5), 185-191.

- Lewicki, P. P. & Wiczowska, J. (2007). Rehydration of apple dried by different methods. *International Journal of Food Properties*, 9(2), 217-226.
- Luengo, E., Álvarez, I., Raso, J. (2013). Improving the pressing extraction of polyphenols of orange peel by pulsed electric fields. *Innovative Food Science and Emerging Technologies*, 17, 79–84.
- Marcone, M. F., Wang, S., Alabish, W., Nie, S., Somnarain, D. & Hill, A. (2013). Diverse food-based applications of nuclear magnetic resonance (NMR) technology. *Food Research International*, 51, 729-747.
- Marigheto, N., Venturi, L., & Hills, B. (2008). Two-dimensional NMR relaxation studies of apple quality. *Postharvest Biology and Technology*, 48, 331–340.
- Marigheto, N., Vial, A., Wright, K., & Hills, B. (2004). A combined NMR and microstructural study of the effect of high pressure processing on strawberries. *Applied Magnetic Resonance*, 26, 521-531.
- Mastrocola, D., Dalla Rosa, M., Massini, R. (1997). Freeze-dried strawberries rehydrated in sugar solutions: mass transfers and characteristics of final products. *Food Research International*, 30(5), 359-364.
- Mauro, M. A, Dellarosa, N., Tylewicz, U., Tappi, S., Laghi, L, Rocculi, P. Dalla Rosa, M. (2015). Calcium and ascorbic acid affect cellular structure and water mobility in apple tissue during osmotic dehydration in sucrose solutions. *Food Chemistry*, *In press*. (doi:10.1016/j.foodchem.2015.04.096)
- Pan, Z., Shih, C., McHugh, T. H., Hirschberg, E. (2008). Study of banana dehydration using sequential infrared radiation heating and freeze-drying. *LWT - Food Science and Technology*, 41, 1944-1951.
- Panarese, V., Laghi, L., Pisi, A., Tylewicz, U. , Dalla Rosa, M., & Rocculi, P. (2012). Effect of Osmotic Dehydration on Actinidia deliciosa Kiwifruit: A Combined NMR and Ultrastructural Study. *Food Chemistry*, 132(4), 1706-1712.
- Puc, M., Corovic, S., Flisar, K., Petkovsek, M., Nastran, J., & Miklavcic, D. (2004). Techniques of signal generation for electroporation. Survey of electroporation devices. *Bioelectrochemistry*, 64, 113-124.
- Quinn, F. X., Kampff, E., Smyth, G., & McBrierty, V. J. (1988). Water in hydrogels 1. A study of water in poly(*N*-vinyl-2-pyrrolidone/methylmethacrylate) copolymer. *Macromolecules* 21, 3191-3198.
- Rastogi, N. K., Eshtiaghi, M.N., & Knorr D. (1999). Accelerated Mass Transfer During Osmotic Dehydration of High Intensity Electrical Field Pulse Pretreated Carrots. *Journal of Food Science*, 64(6), 1020-1023.

- Ratti, C. (2001). Hot air and freeze-drying of high-value foods: a review. *Journal of Food Engineering* 49, 211-319.
- Saldaña, G., Puértolas, E., López, N., García, D., Álvarez, I., & Raso, J. (2009) Comparing the PEF resistance and occurrence of sublethal injury on different strains of *Escherichia coli*, *Salmonella Typhimurium*, *Listeria monocytogenes* and *Staphylococcus aureus* in media of pH 4 and 7. *Innovative Food Science and Emerging Technologies*, 10, 160–165.
- Santagapita, P., Laghi, L., Panarese, V., Tylewicz, U., Rocculi, P., & Dalla Rosa, M. (2013). Modification of Transverse NMR Relaxation Times and Water Diffusion Coefficients of Kiwifruit Pericarp Tissue Subjected to Osmotic Dehydration. *Food and Bioprocess Technology*, 6(6), 1434-1443.
- Taiwo, K. A, Angersbach, A. & Knorr D. (2002). Influence of high intensity electric field pulses and osmotic dehydration on the rehydration characteristics of apple slices at different temperatures. *Journal of Food Engineering*, 52, 185–195.
- Timmermans R.A.H., Nierop Groot M.N., Nederhoff A.L., van Boekel M.A.J.S., Matser A.M. Mastwijk H.C. (2014). Pulsed electric field processing of different fruit juices: Impact of pH and temperature on inactivation of spoilage and pathogenic micro-organisms. *International Journal of Food Microbiology*, 173, 105–111.
- Toepfl, S., Siemer, C., & Heinz, V. (2014). Chapter 8: Effect of High –Intensity Electric Field Pulses on Solid Foods. In Da-Wen Sun (Ed.), *Emerging Technologies for Food Processing* (pp. 147-154).
- Tylewicz, U., Panarese, V., Laghi, L., Rocculi, P., Nowacka, M., Placucci, G., & Dalla Rosa, M. (2011). NMR and DSC Water Study during Osmotic Dehydration of *Actinidia deliciosa* and *A. chinensis* kiwifruit. *Food Biophysics*, 68(2), 327-333.
- Vorobiev E. & Lebovka N. I. (2006). Extraction of intercellular components by pulsed electric fields. In J. Raso & V. Heinz (Eds). *Pulsed electric field technology for food industry: Fundamentals and applications* (pp. 153-193). New York: Springer.
- Vorobiev, E., & Lebovka N. I. (2010). Enhanced extraction from solid foods and biosuspensions by pulsed electrical energy. *Food Eng. Rev.* 2(2), 95–108.
- Wiktor, A., Iwaniuk, M., Śledź, M., Nowacka, M., Chudoba T., & Witrowa-Rajchert D. (2013). Drying Kinetics of Apple Tissue Treated by Pulsed Electric Field. *Drying Technology: An International Journal* 31(1), 112-119.
- Wiktor, A., Schulz, M., Voigt, E., Witrowa-Rajchert, D., Knorr, D. (2015). The effect of pulsed electric fields treatment on immersion freezing, thawing and selected properties of apple tissue. *Journal of Food Engineering*, 146, 8-16.

- Zhang, L., & McCarthy, M.J. (2012). Black heart characterization and detection in pomegranate using NMR relaxometry and MR imaging. *Postharvest Biology and Technology*, 67, 96–100.
- Zhao, J-H., Liu, F., Wen, X., Xiao, H-W., Ni, Y-Y. (2015). State diagram for freeze-dried mango: Freezing curve, glass transition line and maximal-freeze-concentration condition. *Journal of Food Engineering*, 157, 49–56.
- Zimmermann, U. (1996). The effect of high intensity electric field pulses on eucaryotic cell membranes: fundamentals and applications. In U. Zimmermann and G. A. Neil. (Eds.), *Electromanipulation of cells* (pp. 1-106). Boca Raton, CRC Press.
- Zimmermann, U., Pilwat, G., Riemann, F. (1974). Dielectric breakdown of cell membranes. *Biophysical Journal*, 14, 881-899.

ACCEPTED MANUSCRIPT

**Figure Captions**

**Figure 1.** Correlation between cell disintegration index ( $Z_p$ ) and Total Energy delivered to the samples.

**Figure 2.** Correlation between freezable water content ( $x_w^F$ ) and electric field strength applied.

**Figure 3.** Correlation between freezable water content ( $x_w^F$ ) and cell disintegration index ( $Z_p$ ).

**Figure 4.** Example of  $T_1$  distributions (in arbitrary unit, a.u.) obtained on fresh and on two PEF treated samples with 15 pulses at 0.3 and 1.2 kV/cm. The bimodality of the distributions is highlighted in the insets. The first lower inset shows the peak at short relaxation times and the second inset, the peak at long relaxation times. The area under the peak represents the abundance of protons for each population. In this case, the more abundant population is the one at long relaxation times (occupying about the 94% of the total area).

**Figure 5.**  $T_1$  geometric weighted average ( $T_{1g}$ ) and the freezable water ( $x_w^F$ , secondary axis) vs the electric field strength.

**Figure 6.**  $T_1$  peaks position ( $T_{1p}$ ) vs the electric field applied. The bimodality of  $T_1$  distribution has been analysed using the peak at short and at long relaxation times, which are shown separately in the plot.

**Table captions**

**Table 1.** Electric field strength, pulse number, total energy input and disintegration index ( $Z_p$ ) of PEF treated apples.

**Table 2**  $T_{\text{onset}}^f$  and freezable water content ( $x_w^F$ ) average  $\pm$  standard deviation values of untreated and PEF treated apple samples. Statistical significance was assessed by one-way ANOVA. Different letters within the same column indicate statistical differences ( $p < 0.05$ ).

ACCEPTED MANUSCRIPT

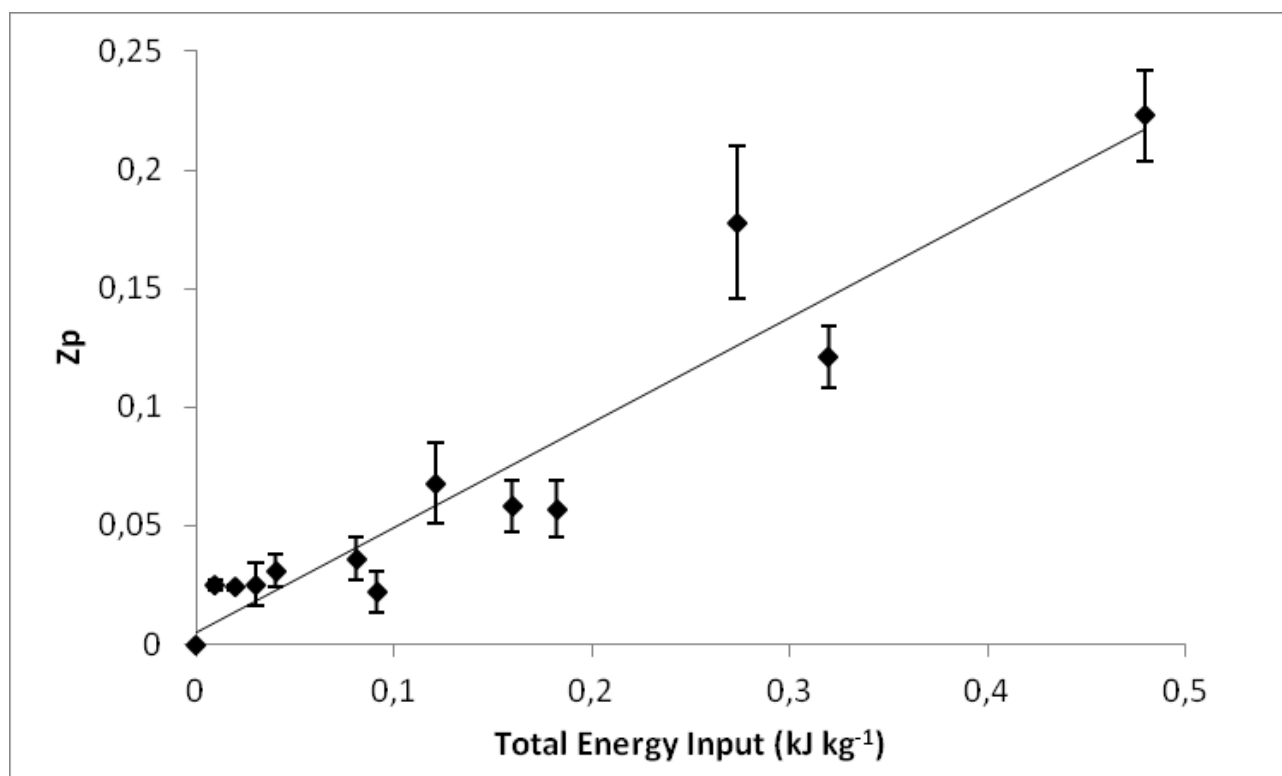


Figure 1

ACCEPTED

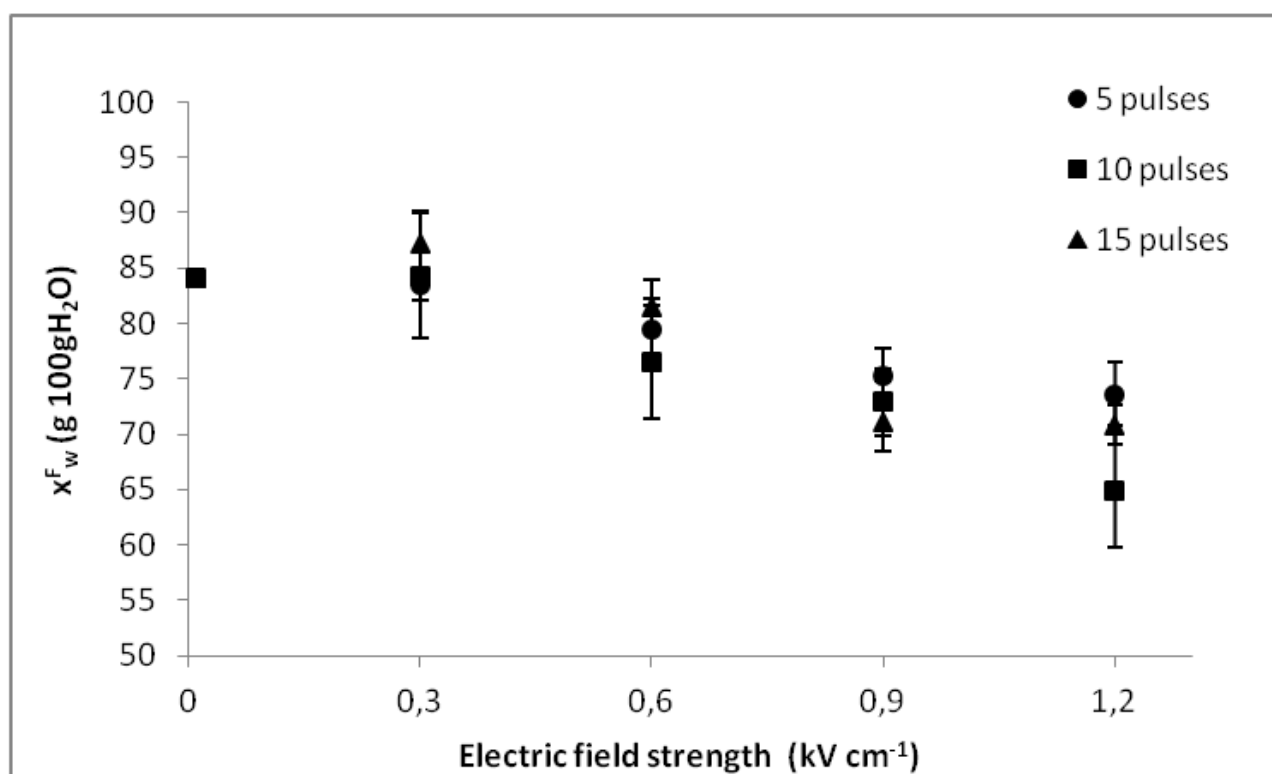


Figure 2

ACCEPTED

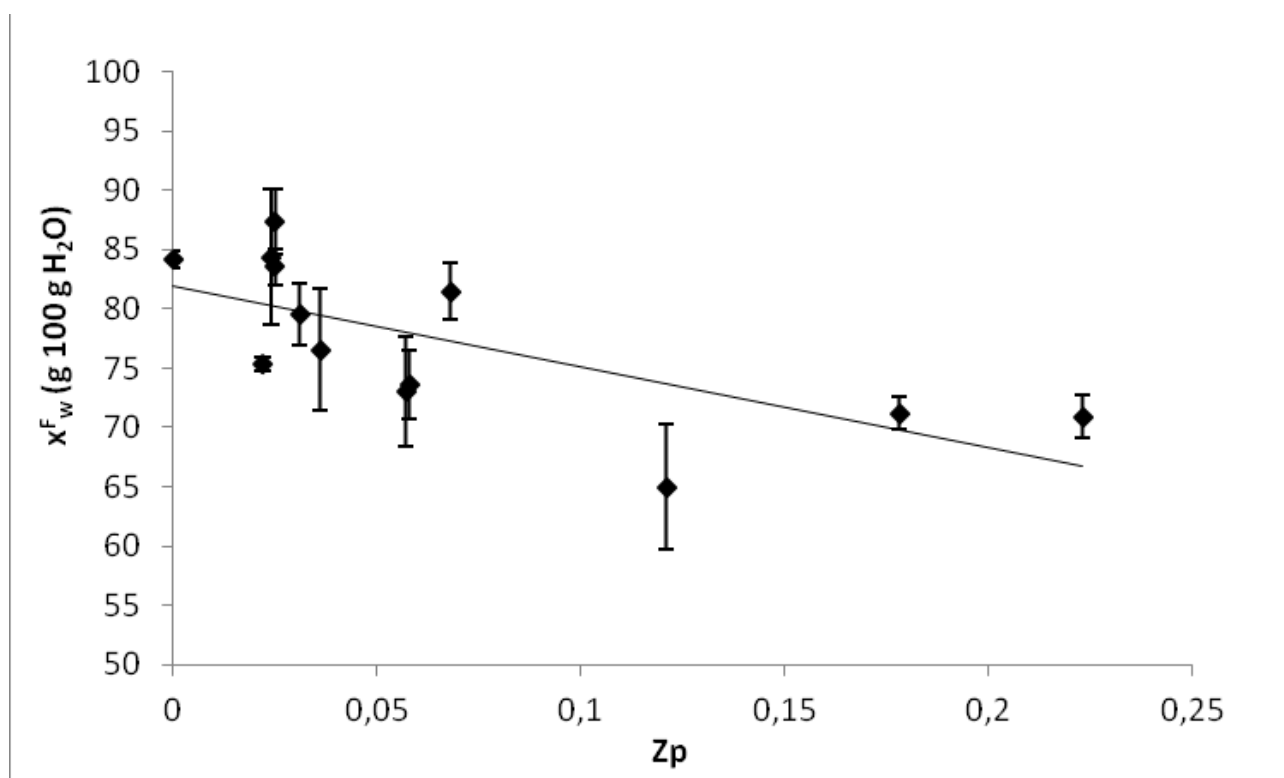


Figure 3

ACCEPTED

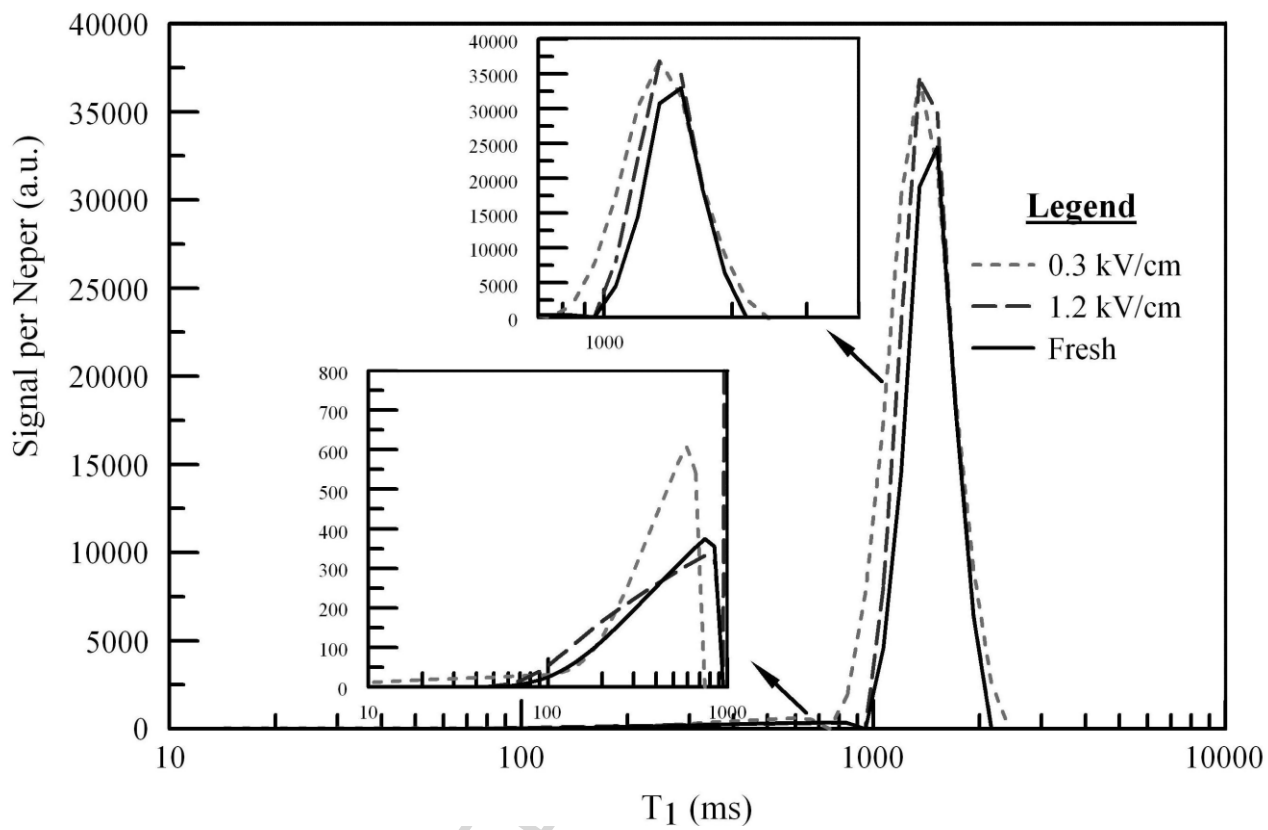


Figure 4

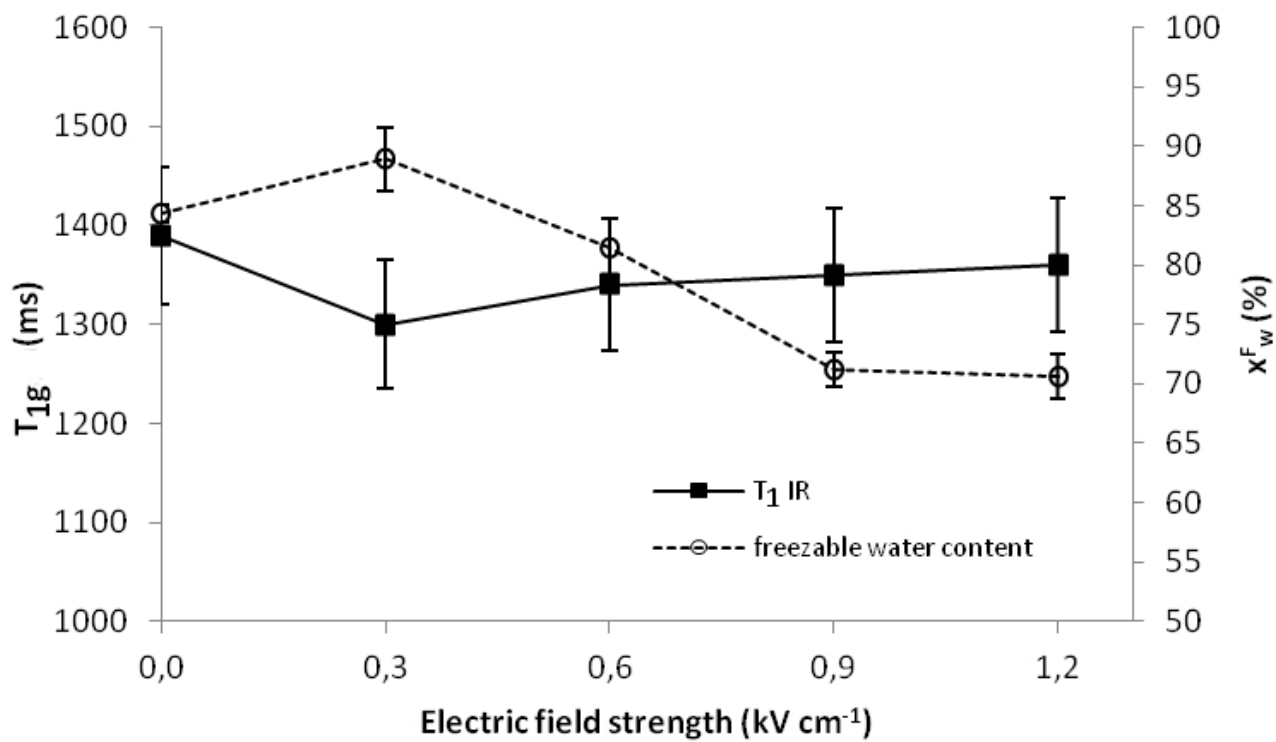


Figure 5

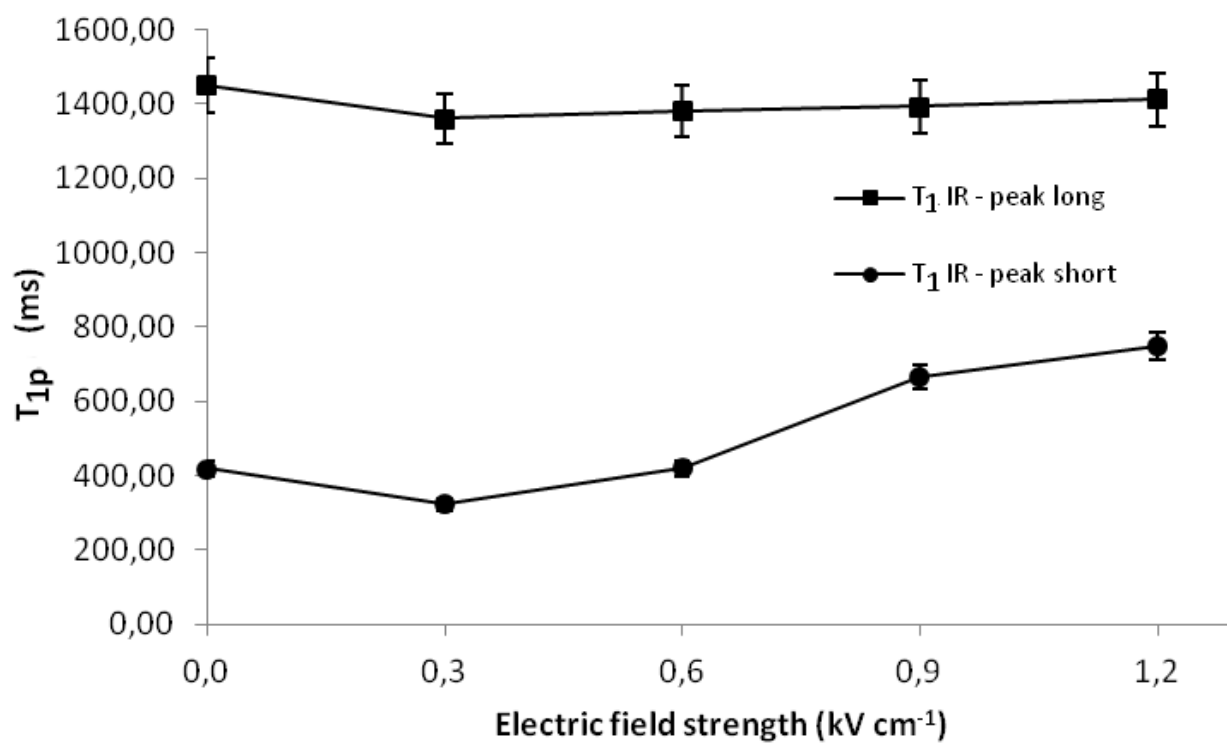


Figure 6

ACCEPTED

Table 1.

| Sample Code | Electric field strength E (kV/cm) | Pulse number ( $\eta$ ) | Total energy input (kJ/kg) | Zp<br>$\bar{x} \pm SD$ |
|-------------|-----------------------------------|-------------------------|----------------------------|------------------------|
| Control     | 0                                 | 0                       | 0                          | 0                      |
| 0.3 p5      | 0.3                               | 5                       | 0.010                      | 0.025 $\pm$ 0.002      |
| 0.3 p10     | 0.3                               | 10                      | 0.019                      | 0.024 $\pm$ 0.001      |
| 0.3 p15     | 0.3                               | 15                      | 0.030                      | 0.025 $\pm$ 0.009      |
| 0.6 p5      | 0.6                               | 5                       | 0.040                      | 0.031 $\pm$ 0.007      |
| 0.6 p10     | 0.6                               | 10                      | 0.081                      | 0.036 $\pm$ 0.009      |
| 0.6 p15     | 0.6                               | 15                      | 0.121                      | 0.068 $\pm$ 0.017      |
| 0.9 p5      | 0.9                               | 5                       | 0.091                      | 0.022 $\pm$ 0.009      |
| 0.9 p10     | 0.9                               | 10                      | 0.182                      | 0.057 $\pm$ 0.012      |
| 0.9 p15     | 0.9                               | 15                      | 0.273                      | 0.178 $\pm$ 0.032      |
| 1.2 p5      | 1.2                               | 5                       | 0.160                      | 0.058 $\pm$ 0.011      |
| 1.2 p10     | 1.2                               | 10                      | 0.320                      | 0.121 $\pm$ 0.013      |
| 1.2 p15     | 1.2                               | 15                      | 0.479                      | 0.223 $\pm$ 0.019      |

Table 2.

| Pulse numbers<br>Voltage<br>(kV/cm) | 5 pulses                     |  | 10 pulses                    |  | 15 pulses                    |  |
|-------------------------------------|------------------------------|--|------------------------------|--|------------------------------|--|
|                                     | T <sub>f onset</sub><br>(°C) | x <sub>w</sub> <sup>F</sup><br>(g·100g <sup>-1</sup> H <sub>2</sub> O) | T <sub>f onset</sub><br>(°C) | x <sub>w</sub> <sup>F</sup><br>(g·100g <sup>-1</sup> H <sub>2</sub> O) | T <sub>f onset</sub><br>(°C) | x <sub>w</sub> <sup>F</sup><br>(g·100g <sup>-1</sup> H <sub>2</sub> O) |
| 0                                   | -8.7 ± 0.8 <sup>a</sup>      | 84.2 ± 0.7 <sup>a</sup>  | -8.7 ± 0.8 <sup>a</sup>      | 84.2 ± 0.7 <sup>a</sup>  | -8.7 ± 0.8 <sup>ab</sup>     | 84.3 ± 0.7 <sup>ab</sup>   |
| 0.3                                 | -8.1 ± 2.8 <sup>a</sup>      | 83.6 ± 1.5 <sup>a</sup>  | -8.7 ± 1.6 <sup>a</sup>      | 84.4 ± 5.7 <sup>a</sup>  | -8.0 ± 0.8 <sup>a</sup>      | 88.9 ± 2.7 <sup>a</sup>  |
| 0.6                                 | -8.9 ± 0.5 <sup>a</sup>      | 79.6 ± 2.6 <sup>ab</sup>   | -9.6 ± 0.9 <sup>a</sup>      | 76.5 ± 5.1 <sup>ab</sup>   | -8.3 ± 1.2 <sup>a</sup>      | 81.5 ± 2.4 <sup>b</sup>  |
| 0.9                                 | -10.5 ± 0.9 <sup>a</sup>     | 75.3 ± 0.6 <sup>b</sup>  | -10.4 ± 1.7 <sup>a</sup>     | 73.1 ± 4.6 <sup>ab</sup>   | -10.8 ± 1.0 <sup>c</sup>     | 71.2 ± 1.4 <sup>c</sup>  |
| 1.2                                 | -10.4 ± 0.7 <sup>a</sup>     | 73.6 ± 2.9 <sup>b</sup>  | -10.6 ± 1.4 <sup>a</sup>     | 64.9 ± 5.2 <sup>b</sup>  | -10.1 ± 0.5 <sup>bc</sup>    | 70.6 ± 1.8 <sup>c</sup>  |

**Highlights:**

- PEF treatment changes the integrity and continuity of the apple cell structure.
- Increasing electric field strength decreases freezable water content.
- Reduction of freezable water content improves product safety.
- Larger volume of PEF-induced water diffusion before relaxing increased  $T_1$  value.

ACCEPTED MANUSCRIPT